*J. Fluid Mech.* (1999), *vol.* 378, *pp.* 335–356. Printed in the United Kingdom



# Transport of reactive tracers in rock fractures

By V. CVETKOVIC[1], J. O. SELROOS[2] AND H. CHENG[1]

[1]Division of Water Resources Engineering, Royal Institute of Technology, Stockholm, Sweden

[2]Swedish Nuclear Fuel and Waste Management Co. (SKB), Stockholm, Sweden

(Received 17 February 1998 and in revised form 10 August 1998)

Transport of tracers subject to mass transfer reactions in single rock fractures is investigated. A Lagrangian probabilistic model is developed where the mass transfer reactions are diffusion into the rock matrix and subsequent sorption in the matrix, and sorption on the fracture surface as well as on gauge (infill) material in the fracture. Sorption reactions are assumed to be linear, and in the general case kinetically controlled. The two main simplifying assumptions are that diffusion in the rock matrix is one-dimensional, perpendicular to the fracture plane, and the tracer is displaced within the fracture plane by advection only. The key feature of the proposed model is that advective transport and diffusive mass transfer are related in a dynamic manner through the flow equation. We have identified two Lagrangian random variables $\tau$ and $\beta$ as key parameteres which control advection and diffusive mass transfer, and are determined by the flow field. The probabilistic solution of the transport problem is based on the statistics of $(\tau, \beta)$, which we evaluated analytically using first-order expansions, and numerically using Monte Carlo simulations. To study $(\tau, \beta)$-statistics, we assumed the 'cubic law' to be applicable locally, whereby the pressure field is described with the Reynolds lubrication equation. We found a strong correlation between $\tau$ and $\beta$ which suggests a deterministic relationship $\beta \sim \tau^{3/2}$; the exponent $3/2$ is an artifact of the 'cubic law'. It is shown that flow dynamics in fractures has a strong influence on the variability of $\tau$ and $\beta$, but a comparatively small impact on the relationship between $\tau$ and $\beta$. The probability distribution for the (decaying) tracer mass recovery is dispersed in the parameter space due to fracture aperture variability.

## 1. Introduction

Deep geological formations, in particular those consisting of crystalline rocks, are generally considered as stable environments suitable for disposal of highly toxic and radioactive wastes. The efficiency of geological media in preventing the spreading of radionuclides from failed canisters to the biosphere depends to a large extent on the mass transfer/retention processes (diffusion and sorption). Most of the radionuclides of interest are sorptive. For the concentrations in question, the capacity of the rock mass for sorption is essentially infinite. However, radionuclides first have to diffuse into the rock in order to access the extensive pool of sorption sites in the rock matrix (Neretnieks 1980). Diffusion in turn depends on the advective transport paths through fractured rock, emphasizing the coupling between flow, advective transport and mass transfer reactions.

Fluid flow and tracer transport in fractured rock take place along distinct conductive features which essentially coincide with fractures. Based on available experimental

data, a fracture in crystalline rock is percieved as a void bounded by two macroscopically planar surfaces that are microscopically (locally) irregular. The opening of the fracture (aperture) varies from point to point in the fracture plane, resulting in two-dimensional heterogeneous flow fields. Tracers injected in fractures of a fluid-saturated rock are advected and dispersed, and are subject to various mass transfer reactions. In particular, the tracers diffuse into the rock matrix and (if reactive) sorb on internal surfaces of the rock. Fractures of crystalline rocks may be filled more or less with gauge (infill) material which further enhances sorption and hence retention.

Various models have been used for describing fluid flow and tracer transport in rock fractures. The basic model for fracture flow is the parallel plate model with laminar (Poiseuille) flow where fluid discharge is proportional to the aperture cubed ('cubic law'). In the simplest form, the entire fracture is percieved as a parallel plate with spatially uniform properties (Snow 1965). Then next level of complexity is to conceptualize flow in fractures as 'channelling' where the parallel plate model is applicable along each channel, but the fracture aperture (or fluid velocity) of each channel varies randomly (e.g. Neuzil & Tracy 1981; Neretnieks 1983); the channel model has been used for interpreting results from tracer experiments both in the laboratory (e.g. Moreno, Neretnieks & Eriksen 1985) and in the field (e.g. Neretnieks, Eriksen & Tähtinen 1982). A further level of complexity is to assume the parallel plate model and the cubic law applicable *locally*, where the fracture aperture is a random space function (RSF) (e.g. Moreno *et al.* 1988; Tsang & Tsang 1989). Simulations of flow and advective transport with variable aperture (e.g. Moreno *et al.* 1988; Tsang & Tsang 1989) have provided important insights into the channelling phenomena, demonstrating the formation of 'preferential' flow paths (channels) as an artifact of the dynamics of flow in strongly varying aperture fields.

Transport in fractures of tracers subject to mass transfer (matrix diffusion and sorption) has been studied in the past using analytical models with a simplified flow configuration (e.g. Neretnieks *et al.* 1982; Neretnieks 1983; Moreno *et al.* 1985; Wels, Smith & Vandergraaf 1994); these models did not explicitly account for the effect of spatial variability in fracture aperture on tracer mass transfer. Similarly, analytical models that account for flow heterogeneity when solving advective transport, do not account for the effect of aperture variability on matrix diffusion (Cvetkovic 1991). The impact of aperture variability on tracer mass transfer (diffusion and sorption) has been accounted for in numerical particle-tracking simulations; however, the dynamics of the flow was not explicitly accounted for (e.g. Moreno & Neretnieks 1993). In spite of various simplifications and limitations, results on flow and reactive transport in fractures obtained in the past clearly demonstrate the significance of heterogeneity for both advective transport and mass transfer processes.

In this paper, we investigate solute transport in single rock fractures, where we consider two key mechanisms: *advection* (i.e. tracer bulk movement along random flow paths) and *mass transfer reactions* (diffusion into the matrix and rate-limited sorption). The Lagrangian framework for transport in aquifers (Cvetkovic & Dagan 1994, 1996; Dagan & Cvetkovic 1996; Cvetkovic, Dagan & Cheng 1998) is in this work extended to single rock fractures. We provide analytical probabilistic solutions where for the first time diffusive mass transfer is related to the dynamics of the flow; the flow field and mass transfer processes are both subject to (strongly) correlated statistical variations due to variations in the fracture aperture. An illustration example emphasizes the effect of aperture heterogeneity on the tracer residence time in the fracture–rock matrix system.

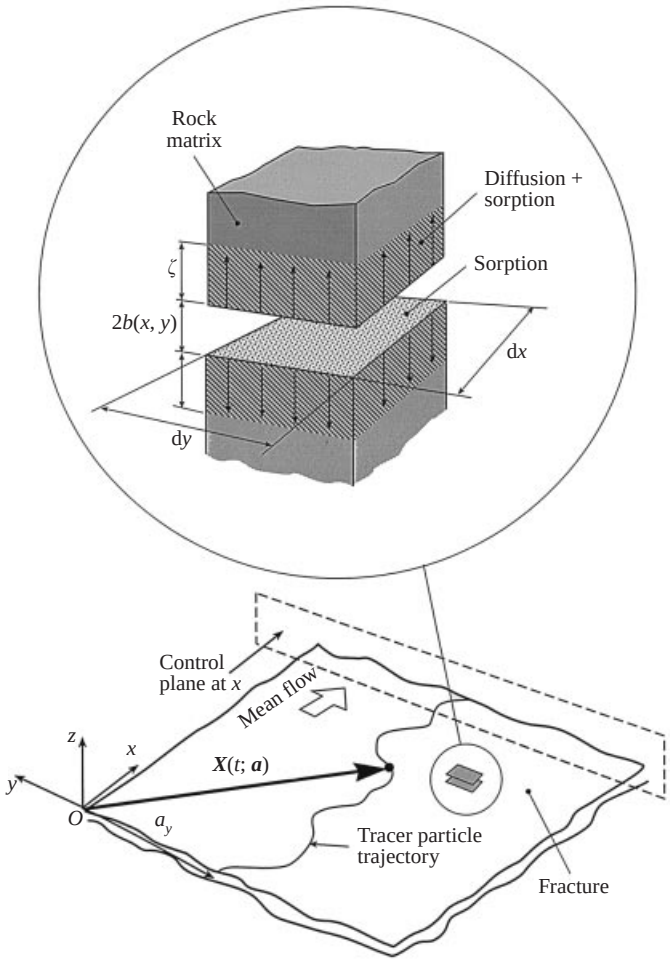


FIGURE 1. Configuration sketch of a tracer particle trajectory in a single fracture originating from $(a_x = 0, a_y)$; an elementary area $\mathrm{d}x \times \mathrm{d}y$ in the fracture with the surrounding rock matrix is also shown.

## 2. Governing equations and assumptions

Conductive features in crystalline rock are conceptualized as essentially two-dimensional voids (fractures) bounded by irregular, planar in the mean, surfaces of the rock (figure 1). The rock, as well as rock fractures, are assumed saturated with water which moves mainly through the fractures. The opening between the two surfaces (aperture) determines the rate of water flow in a fracture, for a given pressure gradient. Let $2b(\boldsymbol{x})$ be the aperture at a given location in the fracture plane $\boldsymbol{x}(x, y)$ (figure 1), where $b$ is the half-aperture and is assumed to be a random space function (RSF). The fracture may contain some infill (gauge) material that in general will not influence fluid flow but can influence mass transfer reactions by enhancing sorption.

A reactive tracer injected at a specified location in the fracture is advected along random flow paths by the fluid flow and dispersed, e.g. due to small-scale velocity variations and/or diffusion, into adjacent streamlines in the fracture plane. In addition, the tracer is generally subject to various mass transfer processes both in the fracture and in the rock matrix.

The governing transport equation can be written in a compact form as

$$\frac{\partial \mathscr{C}}{\partial t} + \nabla \cdot \mathscr{J} - \mathscr{S} = 0 \tag{1}$$

where $\mathscr{C}$ is the vector of mobile and immobile concentrations in the fracture/rock matrix system, $\mathscr{J}$ is the tracer mass flux vector, and $\mathscr{S}$ is the vector of sink/source terms. $\mathscr{S}$ in general depends on $\mathscr{C}$, and a set of parameters that may all be RSFs. The quantities $\mathscr{C}$ and $\mathscr{J}$ are functions of the three-dimensional position $\boldsymbol{x}(x, y, z)$ and time $t$.

In this analysis we consider mass transfer reactions for which the vectors $\mathscr{C}$, $\mathscr{J}$ and $\mathscr{S}$ are defined by

$$\mathscr{C} \equiv \begin{bmatrix} C \\ C_m \\ C' \\ C'_m \end{bmatrix}, \quad \mathscr{J} \equiv \begin{bmatrix} \boldsymbol{J} \\ \boldsymbol{J}_m \\ \boldsymbol{0} \\ \boldsymbol{0} \end{bmatrix}, \quad \mathscr{S} \equiv \begin{bmatrix} \psi \\ \psi_m \\ \psi' \\ \psi'_m \end{bmatrix}, \tag{2}$$

where $C$ $[ML^{-3}]$ is the concentration, $\mathbf{J}$ $[ML^{-2}T^{-1}]$ is the tracer mass flux, and $\psi$ $[ML^{-3}T^{-1}]$ is the source (sink) term; quantities without the index $m$ pertain to the fracture, and quantities with the index $m$ to the rock matrix; quantities without primes pertain to the mobile tracer whereas those with primes pertain to the immobilized tracer, for which by definition the mass flux is zero.

The following mass transfer reactions are to be considered in this study: *diffusion into the rock matrix*, *sorption in the matrix*, *sorption on the fracture surfaces*, *sorption onto gauge material*; in addition, the tracers of interest are generally subject to *decay* and/or possibly irreversible sorption. In order to formulate and solve the transport problem using (1)–(2), we need to specify the mass flux and the sink/source terms, consistent with the mass transfer processes of interest. To specify $\boldsymbol{J}_m$ and the source terms, we adopt the following assumptions:

(i) All mass transfer reactions are linear.

(ii) The movement of tracers in the rock matrix is assumed to be due to molecular diffusion only, i.e. advection in the matrix is neglected; hence $\boldsymbol{J}_m$ is a diffusive flux.

(iii) $\boldsymbol{J}_m(0, 0, J_{mz})$, i.e. diffusion is one-dimensional from the fracture into the rock matrix, where transverse fluxes (i.e. diffusive fluxes parallel to the fracture plane) are neglected (figure 1).

(iv) The mass flux in the fracture is due to advection only.

(v) Fully mixed conditions prevail in the fracture, in the direction orthogonal to the fracture plane (figure 1); hence $C$ and $C'$ are functions of the position in the fracture plane, $\boldsymbol{x}(x, y)$ (figure 1), and time.

The above assumptions provide the basis for transport models that have been used in the past (e.g. Neretnieks *et al.* 1982; Neretnieks 1983; Moreno *et al.* 1985; Cvetkovic 1991; Wels *et al.* 1994). Based on assumptions (i)–(v), transport models of different complexity may be formulated, depending on how fluid flow and the advective mass flux in the fracture are related to mass transfer reactions. Common to all models in the current literature is that the source term $\psi$ in the fracture does not account for the dynamics of the fluid flow. The important issue to be addressed here then is one of relating the tracer mass flux in the fracture, $\boldsymbol{J}$, to the source term in the fracture, $\psi$, in a dynamic manner, i.e. through the flow equation.

The sink/source terms in (1) based on assumptions (i)–(v) are defined as follows:

$$\left.\begin{aligned} \psi &\equiv -\frac{\theta}{b(\boldsymbol{x})}\, J_{mz}(\boldsymbol{x}, z, t)\,|_{z=0} \; -\lambda\, C - \alpha_f\, [K_d^f(\boldsymbol{x})\, C - C'], \\ \psi' &\equiv \alpha_f\, [K_d^f(\boldsymbol{x})\, C - C'] - \lambda\, C', \\ \psi_m &\equiv -\alpha_m (K_d^m\, C_m - C_m') - \lambda\, C_m, \\ \psi_m' &\equiv \alpha_m (K_d^m\, C_m - C_m') - \lambda\, C_m', \end{aligned}\right\} \tag{3}$$

with

$$J_{mz}(\boldsymbol{x}, z, t) = -D\, \frac{\partial C_m}{\partial z}. \tag{4}$$

In (3)–(4), $\theta$ [-] is the porosity of the rock matrix, $D$ $[L^2 T^{-1}]$ is pore diffusivity in the rock matrix ($D\theta$ being the effective diffusivity, $K_d^f$ [-] and $K_d^m$ [-] are dimensionless distribution coefficients for reversible sorption in the fracture and matrix, respectively, $\lambda$ $[T^{-1}]$ is the rate of decay, $\alpha_f$ $[T^{-1}]$ is the rate coefficient for reversible sorption in the fracture, e.g. on the fracture surface and/or in gauge material, and $\alpha_m$ $[T^{-1}]$ is the rate coefficient for reversible sorption in the rock matrix.

The first term in the definition of $\psi$ in (3) is the rate of diffusive mass transfer from the fracture into the rock matrix. The last term of $\psi$ in (3) accounts for first-order reversible sorption–desorption in the fracture, and the corresponding term in the definition of $\psi_m$ for first-order reversible sorption–desorption in the rock matrix. Note that (3)–(4) implies symmetry in the diffusion process in the $z$-direction.

The most important generalization in (3)–(4) compared to the models used in the past (e.g. Neretnieks *et al.* 1982; Neretnieks 1983; Moreno *et al.* 1985; Wels *et al.* 1994) is that the advective tracer flux $\boldsymbol{J}$ and the source term in the fracture, $\psi$, are related in a dynamic manner through the two-dimensional flow equation (A 1) (Appendix A).

For a given realization of the RSF $b(\boldsymbol{x})$, the two-dimensional fluid velocity $\boldsymbol{V}(V_x, V_y)$ is computed from the pressure field which is obtained from the Reynolds lubrication equation (A 1) (Appendix A), with specified steady-state boundary conditions. Hence, we assume the 'cubic law' to be applicable *locally* over an element $\mathrm{d}x \times \mathrm{d}y$ (figure 1). The tracer mass flux for pure advection in the fracture (assumption (iv)) is defined by

$$\boldsymbol{J}(\boldsymbol{x}, t) = C(\boldsymbol{x}, t)\, \boldsymbol{V}(\boldsymbol{x}). \tag{5}$$

Even for a chemically inert tracer with $K_d^f = K_d^m = 0$, diffusion into the matrix as well as decay may take place; thus in the present context, 'reactive' is used in a general sense designating chemical and/or physical interactions with the rock matrix or fracture surface, including decay. 'Non-reactive' tracer thus implies an *idealized* tracer, or marked fluid, subject to advection only.

The parameters $K_d^m$ and $\alpha_m$ in (3) reflect uniform sorption properties of the rock matrix. The parameters $K_d^f$ and $\alpha_f$ reflect sorption properties of the infill (gauge) material and/or of the fracture surface. These are generally subject to random variations, say due to variations in the density of gauge material, or the variations in the aperture. Field data on the sorption rate $\alpha_f$ are limited; at most, one can obtain a rough estimate of its effective (mean) value. Moreover, recent studies of reactive transport in aquifers show that the impact of spatial variability of the rate coefficient corresponding to $\alpha_f$ is limited; the most significant are the mean values (e.g. Cvetkovic *et al.* 1998). Thus, we consider $\alpha_f$ in (3) to be spatially uniform.

Our specific goal here is to develop deterministic and probabilistic solutions of the equation system (1)–(2) with (3)–(5), for specified initial and boundary conditions. In the next Section, we derive Lagrangian transport equations. In § 4 a general solution to the Lagrangian transport problem is derived in the Laplace domain for a pulse input, and limiting cases are presented in Laplace and real domains. Probabilistic solutions are given in § 5 and § 6 and illustrated in § 7.

## 3. Lagrangian transport formulation

In order to solve the reactive transport problem in a fracture, we shall transform the Eulerian transport equations (1)–(2) using Lagrangian coordinates; the methodology to be used here is the one developed by Cvetkovic & Dagan (1994).

A conservative (non-reactive) and dynamically inert tracer injected at $\boldsymbol{a}(0, a_y)$ (figure 1) is advected as an indivisible entity; we refer to it as a tracer parcel, or particle. The parcel advection trajectory is $\boldsymbol{X}(t;\boldsymbol{a})$ $[X_x(t;\boldsymbol{a}), X_y(t;\boldsymbol{a})]$, with $\boldsymbol{X}(0;\boldsymbol{a}) = \boldsymbol{a}$, where $\boldsymbol{X}$ is obtained by solving $\mathrm{d}\boldsymbol{X}(t;\boldsymbol{a})/\mathrm{d}t = \boldsymbol{V}[\boldsymbol{X}(t;\boldsymbol{a})]$ (Taylor 1921; Dagan 1984).

A useful parametrization of Lagrangian variables is in terms of $x$, i.e. the position parallel to the mean flow. The solution of $x - X(t;\boldsymbol{a}) = 0$ yields $t = \tau(x;\boldsymbol{a})$ where $\tau = 0$ for $a_x = 0$. Hence $\tau$ is the advective travel time from $a_x (= 0)$ to $x$. If $x - X(t;\boldsymbol{a}) = 0$ has multiple roots, we select the first passage time. Next we define $\eta(x;\boldsymbol{a}) = X_y(\tau;\boldsymbol{a})$ where $y = \eta$ pertains to the trajectory. The Lagrangian quantities $\tau$ and $\eta$ satisfy differential equations $\mathrm{d}\tau/\mathrm{d}x = 1/V_x(x,\eta)$ and $\mathrm{d}\eta/\mathrm{d}x = V_y(x,\eta)/V_x(x,\eta)$ with $\eta(0;\boldsymbol{a}) = a_y$.

With the transformation $\xi \equiv y - \eta$, $\mathscr{C}(\boldsymbol{x}, t)$ in (1)–(2) become Lagrangian variables $\mathscr{C}(t, \tau; a_y)$; for simplicity, we retain the same notation for Eulerian and Lagrangian quantities. Transforming all quantities in (1)–(2) and (3)–(5) yields a Lagrangian mass balance equation system which pertains to a trajectory originating from $\boldsymbol{a}$:

$$\left.\begin{aligned} \frac{\partial C}{\partial t} + \frac{\partial C}{\partial \tau} &= \frac{\theta D}{b(\tau)} \frac{\partial C_m}{\partial z}\bigg|_{z=0} - \lambda C - \alpha_f [K_d^f(\tau) C - C'], \\ \frac{\partial C_m}{\partial t} &= D \frac{\partial^2 C_m}{\partial z^2} - \alpha_m (K_d^m C_m - C_m') - \lambda C_m, \\ \frac{\partial C'}{\partial t} &= \alpha_f [K_d^f(\tau) C - C'] - \lambda C', \\ \frac{\partial C_m'}{\partial t} &= \alpha_m (K_d^m C_m - C_m') - \lambda C_m'. \end{aligned}\right\} \tag{6}$$

The advective residence time $\tau(x;\boldsymbol{a})$ can be written in an integral form as

$$\tau(x;\boldsymbol{a}) = \int_{a_x=0}^{x} \frac{\mathrm{d}x'}{V_x[x', \eta(x';\boldsymbol{a})]}. \tag{7}$$

The boundary conditions are prescribed as

$$\left.\begin{aligned} C &= C_m \quad \text{at} \quad z = 0, \\ C_m &= 0 \quad \text{or} \quad \frac{\partial C_m}{\partial z} = 0 \quad \text{at} \quad z = \zeta, \\ C(t,0) &= C_0(t) \quad \text{at} \quad x = 0 \quad \text{or} \quad \tau = 0, \end{aligned}\right\} \tag{8}$$

where we consider two types of boundary conditions for $C_m$: zero concentration ($C_m = 0$), and zero flux ($\partial C_m/\partial z = 0$). Zero initial condition is assumed for all concentrations.

An example of a physical situation for which the zero flux boundary condition ($\partial C_m/\partial z = 0$) would be appropriate is a system of three fractures in which tracer transport occurs simultaneously in all three and we model the transport in the middle fracture; $\zeta$ is then half the distance from the middle fracture to either one of the other two fractures. The zero concentration boundary condition ($C_m = 0$) would be appropriate in the same situation of three fractures, provided that tracer transport occurs solely in the middle fracture. Then the other two fractures act as sinks for the tracer, once the tracer has diffused to $\zeta$ which here is the distance between fractures. The latter situation is more likely to occur in reality, where the lenght $\zeta$ is a known (linear) function of distance. For simplicity, we assume the three fractures to be parallel, hence $\zeta$ is uniform.

Most common injection and detection modes in applications are given in terms of the tracer mass flux $[ML^{-2}T^{-1}]$, or the tracer discharge $[MT^{-1}]$. The transport is then described as the tracer breakthrough (i.e. mass flux or discharge) at a control plane at $x$, orthogonal to the mean flow (figure 1).

Let $q$ $[MT^{-1}]$ denote tracer discharge at the location $x$. Then $q = CV_1\Delta A = J_x\,\Delta A$, where $\Delta A$ is the infinitesimal cross-sectional area in the control plane $(y, z)$ at $x$ over which the tracer is discharged (figure 1). Since the mass transfer processes considered are linear, the basic solution of the transport problem is obtained for a pulse (instantaneous) injection, i.e. $C(t, 0) = (C_0\Delta t_0)\ \delta(t)$, where $\Delta t_0$ is the infinitesimal time interval of injection, $C_0$ is the tracer concentration of the injected solution, and $\delta$ is the Dirac delta function. If the injected solution volume is $\Delta\mathscr{V}$, the total injected mass is $\Delta M = C_0\,\Delta\mathscr{V}$. The solution for the tracer concentration, $C$, and tracer discharge, $q$, is then (Cvetkovic & Dagan 1994)

$$C(t, \tau) = C_0\Delta t_0\,\gamma(t, \tau), \quad q(t, \tau) = \Delta M\,\gamma(t, \tau). \tag{9}$$

With $\Delta M$ given, the focus of our analysis is on the function $\gamma$ $[T^{-1}]$. For tracer injection over finite time intervals with a given rate function, the solution for $q$ is obtained by convolution.

## 4. Solution for a single flow path

The solution of the system (6) with boundary conditions (8) and for zero flux (i.e. $\partial C_m/\partial z = 0$) at $z = \zeta$, is obtained in the Laplace domain as (Appendix B)

$$\widehat{q}/\Delta M \equiv \widehat{\gamma} = \exp\left[-\tau s' - \beta\,\theta(D\,G_m(s'))^{1/2}\,A(s') - \frac{s'}{s'/\alpha_f + 1}\int_0^\tau K_d^f(\epsilon)\,\mathrm{d}\epsilon\right], \tag{10}$$

where

$$G_m(s) \equiv s\left(1 + \frac{K_d^m}{s/\alpha_m + 1}\right), \quad A(s) \equiv \frac{\exp\left[2\,\zeta\,(D^{-1}\,G_m)^{1/2}\right] - 1}{\exp\left[2\,\zeta\,(D^{-1}\,G_m)^{1/2}\right] + 1}, \quad s' \equiv s + \lambda, \tag{11}$$

and

$$\beta(\tau) = \int_0^\tau \frac{\mathrm{d}\tau'}{b(\tau')}. \tag{12}$$

$G_m$ accounts for the kinetic sorption in the rock matrix, $A$ accounts for the effect of a limited diffusion zone on matrix diffusion, and the last term in the exponential (10) accounts for the kinetic sorption in the fracture; note that sorption in the rock matrix takes place only after the tracer has diffused into it from the fracture. The solution

for the zero concentration boundary condition (i.e. $C_m = 0$) at $z = \zeta$ is identical to (10), except that the function $A$ is replaced by $A^{-1}$ (Appendix B).

Surface sorption is typical for fractures in crystalline rocks. $K_d^f \sim 1/b$ is a common assumption (e.g. Moreno *et al.* 1985), and we can write $K_d^f(\boldsymbol{x}) = K_a/b(\boldsymbol{x})$, where $K_a$ $[L]$ is a spatially uniform distribution coefficient for reversible surface sorption (once equilibrium is reached). Note that in some cases $K_d^f(\boldsymbol{x}) = K_a/b(\boldsymbol{x})$ with $K_a$ uniform may not be applicable (Wels *et al.* 1994); we may then consider $K_d^f$ as a RSF correlated to $b$, or use an alternative functional form between $K_d^f$ and $b$. Furthermore, for many applications $\zeta$ may be considered as sufficiently large such that the influence of the boundary at $\zeta$ is small; thus we shall simplfy the solution by assuming $\zeta \to \infty$.

With $K_d^f(\tau) = K_a/b(\tau)$, and $\zeta \to \infty$ (whereby $A \to 1$), the solution (10) becomes:

$$\widehat{\gamma} = \exp\left[-\tau s' - \beta\,\theta(D\,G_m(s'))^{1/2} - \beta G_f(s')\right], \tag{13}$$

where

$$G_f(s) \equiv s\left(\frac{K_a}{s/\alpha_f + 1}\right). \tag{14}$$

Using $\mathrm{d}\tau = \mathrm{d}x/V_x$ and $\tau = \tau(x)$, we can write $\beta$ (12) as

$$\beta(x) = \int_{a_x=0}^{x} \frac{\mathrm{d}x'}{V_x[x', \eta(x')]\, b[x', \eta(x')]}. \tag{15}$$

The parameters $K_d^m, K_a, D, \theta, \alpha_m, \alpha_f$ in (13) can in principle be determined in the laboratory from rock samples. $\beta$ (12) is a new Lagrangian quantity that controls mass transfer along a flow path (streamtube) and depends on the flow field. Equation (12) establishes a nonlinear relationship between $\tau$ and $\beta$, which for a given realization of the RSF $b(\boldsymbol{x})$ can be solved numerically (see § 6.3). The quantities $\tau$ and $\beta$ are (correlated) random variables, due to the randomness of $\boldsymbol{V}(\boldsymbol{x})$, i.e. of the aperture $2b(\boldsymbol{x})$. Note that for a given RSF $b(\boldsymbol{x})$, and given parameters $K_d^m, K_a, D, \theta, \alpha_m, \alpha_f$, diffusion can be influenced only by changing the boundary condition for the flow. If the fracture is approximated as uniform with $b = const.$, then $\beta$ (15) can be expressed as the ratio of the surface area of a uniform 'channel' through which transport takes place, and the volumetric flow rate of the 'channel'; hence reference to $\beta$ for uniform fractures as 'flow-wetted surface' (Moreno & Neretnieks 1993) or 'specific surface area' (Wels *et al.* 1994).

The function $\gamma(t, \tau)$ that is obtained by inverting (10) or (13), and is suitably normalized if $\lambda \neq 0$, may be interpreted as a probability density function of *subparticle residence time*, $\vartheta$. The concept of 'subparticles' has been used recently for describing non-reactive transport by groundwater (Dagan & Fiori 1997). The tracer parcel (or particle) injected at a location $\boldsymbol{x} = \boldsymbol{a}$ can be viewed as consisting of many indivisible 'subparticles' (e.g. molecules). In the absence of mass transfer processes, the tracer parcel is advected as an indivisible entity. Due to mass transfer reactions, however, the tracer parcel is 'deformed,' or dispersed, whereby the subparticles diffuse into the rock matrix, are sorbed in the fracture and in the rock matrix, and in addition can 'disappear' due to decay and/or irreversible sorption. For given advection (i.e. fixed $\tau$), normalized $\gamma(t, \tau)$ quantifies the probability that a subparticle will cross the control plane at $x$ within the time interval $\mathrm{d}t$ at time $\vartheta = t$. The subparticles are retarded by mass transfer processes, relative to the advective movement of the tracer parcel; in the absence of mass transfer, $\gamma = \delta(t - \tau)$, and all subparticles arrive at $x$ and $y = \eta$ at $\vartheta = t = \tau$ with probability 1.

Several limiting cases of interest for applications can be obtained from (13). The

simplest case is when all mass transfer reactions are absent, i.e. $D = K_d^m = K_a = 0$; (13) then reduces to $\hat{\gamma}(s,\tau) = \exp(-s'\tau)$, the inversion of which yields advection with decay, i.e. $\gamma(t,\tau) = \exp(-\lambda t)\,\delta(t-\tau)$.

In the absence of matrix diffusion ($D = 0$), sorption is possible in the fracture only. If sorption is sufficiently fast (equilibrium) with $\alpha_f \to \infty$, $G_f = s' K_a$, and (13) reduces to

$$\hat{\gamma}(s,\tau;\beta) = \exp\left(-s'\tau - s'\beta K_a\right). \tag{16}$$

Inversion of (16) yields retarded advection with decay

$$\gamma(t,\tau;\beta) = \exp(-\lambda t)\,\delta(t-\tau-K_a\beta). \tag{17}$$

If sorption in the fracture is kinetically controlled, i.e. $\alpha_f$ is finite, then

$$\hat{\gamma}(s,\tau;\beta) = \exp\left[-s'\tau - \beta\, G_f(s')\right], \tag{18}$$

the inversion of which yields

$$\gamma(t,\tau;\beta) = \mathrm{e}^{-\alpha_f K_a\beta-\lambda t}\delta(t-\tau)+\alpha_f^2 K_a\beta\exp\{-\alpha_f[K_a\beta+(t-\tau)]-\lambda t\}\,\tilde{I}_1[\alpha_f^2 K_a\beta(t-\tau)], \tag{19}$$

where $\tilde{I}_1(Z) \equiv I_1(2Z^{1/2})/Z^{1/2}$ with $I_1$ being the modified Bessel function of the first kind of order one. A model analogous to (19) with $K_a\beta \to \tau K_d$ is common for describing sorption in aquifers and soils (e.g. Cvetkovic & Dagan 1994; Destouni & Cvetkovic 1991).

If both diffusion and sorption (in the rock matrix and on fracture surfaces) take place, and equilibrium prevails both in the fracture and matrix, i.e. $\alpha_m$, $\alpha_f \to \infty$, we have

$$\hat{\gamma}(s,\tau;\beta) = \exp\left[-s'\,(\tau+\beta K_a) - \beta\,\theta\,(DR_m\,s')^{1/2}\right]. \tag{20}$$

Inversion of (20) yields

$$\gamma(t,\tau;\beta) = \frac{H(t-\tau)\,\beta\,\theta\,(DR_m)^{1/2}}{2\pi^{1/2}(t-\tau-\beta K_a)^{3/2}}\,\exp\left[\frac{-\beta^2\,\theta^2\,D\,R_m}{4(t-\tau-\beta K_a)} - \lambda t\right], \tag{21}$$

where $H(\cdot)$ is the Heaviside step function, and $R_m \equiv 1 + K_d^m$ is the retardation factor in the rock matrix.

If equilibrium prevails in the rock matrix only ($\alpha_m \to \infty$), then $G_m = s'(1+K_d^m) \equiv s'\,R_m$, and

$$\hat{\gamma}(s,\tau;\beta) = \exp\left[-s'\tau - \beta G_f(s') - \beta\,\theta\,(DR_m\,s')^{1/2}\right]. \tag{22}$$

Inversion of (22) yields a convolution integral between (19) and (21).

For cases where $\hat{\gamma}$ cannot be inverted analytically, we can in principle reconstruct $\gamma$ by means of temporal moments. Temporal moments of order $k$ for pulse injection, for instance, are defined by

$$m_k(\tau) \equiv \int_0^\infty t^k\,q\,\mathrm{d}t = \Delta M\int_0^\infty t^k\,\gamma\,\mathrm{d}t = \Delta M\,(-1)^k\frac{\partial^k\hat{\gamma}}{\partial s^k}\bigg|_{s=0}, \tag{23}$$

where $\Delta M$ is the injected tracer mass and $\hat{\gamma}$ is defined in (22). Central temporal moments are readily computed using $m_k$ (23).

## 5. Probabilistic solutions

Due to random variations of the half-aperture, $b(\boldsymbol{x})$, the fluid velocity $\boldsymbol{V}$ is random, and consequently the Lagrangian quantities integrated over the flow path, such as $\tau$

and $\beta$, are random; the solution $\gamma$ is then also random and needs to be quantified statistically. In the cases where $\widehat{\gamma}$ cannot be inverted, the statistics of $\gamma$ can in principle be reconstructed from the statistics of the temporal moments (23). In the general case with $\widehat{\gamma}$ (10), the resulting moments would depend on $\tau$, and on integrals over the $\tau$-domain, that are random. In the case where $\widehat{\gamma}$ is given by (13), $m_k$ (23) depends on $\tau$ and $\beta$, whereby the statistics of the temporal moments can be directly related to the statistics of $\beta$ and $\tau$. In § 7 we illustrate the computation of the PDF of the zero-order temporal moment.

In the cases where a closed-form analytical expression for $\gamma$ is available, tracer breakthrough (or discharge) at location $x$ with advective residence time $\tau(x)$ is quantified by $\gamma$, conditioned on the random variables $\tau$ and $\beta$. We can then compute the mean and variance of $\gamma$ by using the joint PDF of $\tau$ and $\beta$.

Let $f_{\tau\beta} \equiv f(\tau, \beta)$ denote a joint probability density function (PDF) for $\tau, \beta$, at the control plane. The expected $\gamma$ is then evaluated by

$$\langle \gamma \rangle = \int \gamma \, f(\gamma) \, \mathrm{d}\gamma = \int_0^\infty \int_0^\infty \gamma(t, \tau; \beta) \, f(\tau, \beta; x) \, \mathrm{d}\tau \, \mathrm{d}\beta. \tag{24}$$

The variance is defined as $\sigma_\gamma^2 \equiv \langle \gamma^2 \rangle - \langle \gamma \rangle^2$, where $\langle \gamma^2 \rangle$ is evaluated by

$$\langle \gamma^2 \rangle = \int \gamma^2 \, f(\gamma) \, \mathrm{d}\gamma = \int_0^\infty \int_0^\infty \gamma^2(t, \tau; \beta) \, f(\tau, \beta; x) \, \mathrm{d}\tau \, \mathrm{d}\beta. \tag{25}$$

Similarly, we may compute higher-order moments of $\gamma$. The expected tracer discharge $\langle q \rangle$ and the variance of $q$, $\langle q^2 \rangle - \langle q \rangle^2$, are then proportional to $\langle \gamma \rangle$ and $\langle \gamma^2 \rangle - \langle \gamma \rangle^2$, respectively, in view of (9).

## 6. Statistics of $\tau$ and $\beta$

In § 4 we found that $\tau$ and $\beta$ are the two fundamental (Lagrangian) random variables for advection and mass transfer processes in fractures. The probabilistic solutions of the transport problem require knowledge of the joint PDF $f(\tau, \beta)$, as a function of the Eulerian flow statistics. In the following, we first discuss the statistics of the RSF $b(\boldsymbol{x})$. Then we derive the first few moments of $\tau, \beta$ as functions of the flow statistics, based on first-order expansions, and compare them to results of Monte Carlo simulations.

### 6.1. *Aperture variations*

Detailed analysis of single fractures have been performed under laboratory conditions. Different methods for analysing the void space are available; e.g. surface topography, resin injection, and casting methods. Hakami (1995) and Hakami & Larsson (1996) have studied two different type of fractures, a minor fault (highly conductive single fracture) and a well mated joint, respectively, from the Äspö Hard Rock Laboratory in Sweden using injection/photograph techniques. Their results, as well as those of a few other studies, indicate that the spatially variable geometric aperture may be described by a univariate log-normal distribution combined with a two-point spatial correlation function (e.g. exponential variogram) (Hakami 1995; Hakami & Larsson 1996); other types of statistical models are not excluded, however, since experimental data are sparse.

For illustrative purposes, we assume the half-aperture $b$ as log-normally distributed with a exponential correlation structure, i.e.

$$b(\boldsymbol{x}) = b_G \, \mathrm{e}^{Y(\boldsymbol{x})}, \quad C_Y(\boldsymbol{r}) = \sigma_Y^2 \, \exp(-r/I_Y), \tag{26}$$

where $r \equiv |\boldsymbol{r}|$ is the separation distance, $b_G$ is the geometric mean, $Y$ is a normally distributed RSF of zero mean and $I_Y$ is the (isotropic) integral scale of $Y$.

### 6.2. *Analytical results*

Using first-order expansions, expressions for the first two moments of $\tau$ and $\beta$, as well as the joint moment of $\tau$ and $\beta$, are derived in Appendix C.

The mean of $\tau$ and $\beta$ are at first-order

$$\langle\tau\rangle = \tau_0 \frac{x}{I_Y}, \quad \langle\beta\rangle = \beta_0 \frac{x}{I_Y} = \frac{\tau_0}{b_G}\frac{x}{I_Y} = \frac{\langle\tau\rangle}{b_G}, \tag{27}$$

where the normalization constants $\tau_0$ and $\beta_0$ are given in (C 6) of Appendix C.

The variances and the joint moment of $\tau$ and $\beta$ are (Appendix C)

$$\left.\begin{aligned}
\frac{\sigma_\tau^2}{\tau_0^2} &= 8x' - 7\ln x' + 2\mathrm{e}^{-x'} + 7\mathrm{Ei}(-x') + 3\left[\frac{(1+x')\mathrm{e}^{-x'}-1}{x'^2}\right] - \tfrac{1}{2} - 7E,\\
\frac{\sigma_\beta^2}{\beta_0^2} &= 18x' - 11\ln x' + 8\mathrm{e}^{-x'} + 11\mathrm{Ei}(-x') + 3\left[\frac{(1+x')\mathrm{e}^{-x'}-1}{x'^2}\right] - \tfrac{13}{2} - 11E,\\
\frac{\sigma_{\tau\beta}}{\tau_0\beta_0} &= 12x' - 9\ln x' + 4\mathrm{e}^{-x'} + 9\mathrm{Ei}(-x') + 3\left[\frac{(1+x')\mathrm{e}^{-x'}-1}{x'^2}\right] - \tfrac{5}{2} - 9E,
\end{aligned}\right\} \tag{28}$$

where $x' \equiv x/I_Y$, and $E = 0.577\ldots$ is the Euler constant.

### 6.3. *Simulation results*

The aperture $2b$ controls on the one side the flow field, and on the other side diffusive mass transfer between the fracture and rock matrix. For a given hydraulic gradient applied on the fracture, the two-dimensional fluid velocity field is a RSF. The solution of the flow field as described in Appendix A provides the basis for solving the reactive transport problem.

We simulate advective transport in a statistically isotropic heterogeneous fracture with (26) applicable. A constant head is assumed at the boundaries $x/I_Y = -6$ and $x/I_Y = 18$, and no-flow condition is assumed at $y/I_Y = -9$ and $y/I_Y = 9$. The simulation domain is discretized into $96 \times 72$ blocks, with 4 blocks per integral scale. To minimize the effects of boundaries (Rubin & Dagan 1988, 1989), an inner domain is defined within which the particle transport is investigated. The RSF $Y$ is generated using a recently developed method (Bellin & Rubin 1996), and the flow equation (A 1) (Appendix A) is solved by a finite difference method.

A series of Monte Carlo simulations is performed for different values of $\sigma_Y$. A typical streamline field for $\sigma_Y = 0.3$ is shown in figure 2(*a*). The streamlines tend to converge into dominant flow paths. This tendency is even more pronounced in figure 2(*b*) for $\sigma_Y = 0.5$ where a few major ('preferential') flow paths account for most of the fluid flow. This is qualitatively consistent with results from field experiments which indicate that flow in fractures is often 'channellized', i.e. relatively small sections of the fracture provide for most of the flow (e.g. Neretnieks 1993). Similar features have been observed in numerical simulations of flow in single fractures with variable aperture (e.g. Moreno *et al.* 1988; Tsang & Tsang 1989) as well as in two-dimensional, strongly heterogeneous aquifers (e.g. Cvetkovic, Cheng & Wen 1996).

Once the random flow field is established, a single tracer particle is injected into the domain at the origin (i.e. $a_x = a_y = 0$) and is tracked in each realization. The quantities $\tau$, $V_x$, and $b$ are computed along a flow path at different cross-sections ($x$) of the flow domain in each realization. The statistics of $\beta$, $\tau$, are calculated as

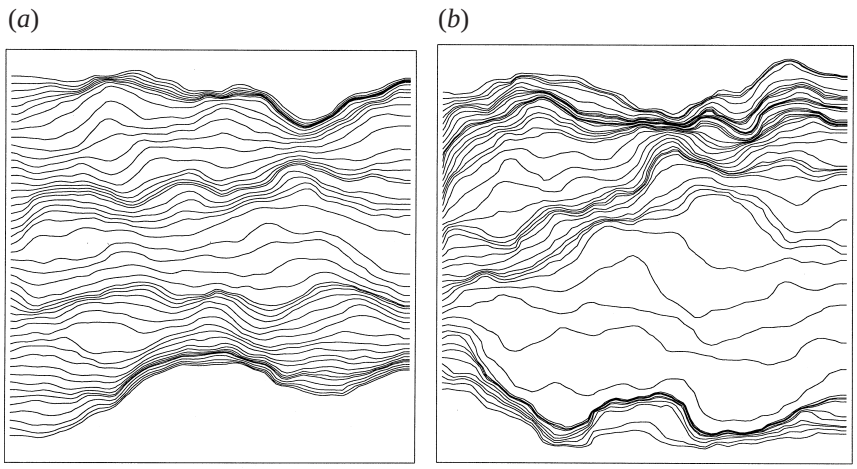


FIGURE 2. A typical realization of a simulated streamline field in a single fracture for: (*a*) $\sigma_Y = 0.3$, and (*b*) $\sigma_Y = 0.5$.

functions of $x/I_Y$. The number of realizations essentially depends on the magnitude of $\sigma_Y$, and is between 1000 and 6000. For comparative purposes, we assume $\tau$ and $\beta$ to be log-normally distributed, and use the analytical model (C 10)–(C 11) of Appendix C.

The simulated and analytical expected values of $\ln\tau$ and $\ln\beta$ are compared in figures 3(*a*) and 3(*b*), respectively. First-order expressions for $\langle\ln\tau\rangle$ and $\langle\ln\beta\rangle$ do not depend on $\sigma_Y$. The discrepancy between the simulated and analytical values seems to decrease with distance (figure 3*a,b*). The arithmetic mean of $\beta$, $\langle\beta\rangle$, (which is not shown in the figures but the simulated values can be closely estimated from figures 3(*b*) and 3(*d*) by assuming a log-normal distribution for $\beta$) is about 25% larger for $\sigma_Y = 0.5$ than for $\sigma_Y = 0.1$. This implies that for a single particle, diffusion into the rock matrix is in a statistical sense enhanced by increasing variability of the fracture aperture.

The log-variances for $\tau$ and $\beta$, $\sigma^2_{\ln\tau}$ and $\sigma^2_{\ln\beta}$, obtained from simulations, are illustrated and compared to analytical results in figures 3(*c*) and 3(*d*), respectively. A strong dependence of both $\sigma^2_{\ln\tau}$ and $\sigma^2_{\ln\beta}$ on the aperture variability is apparent. The analytical first-order $\sigma^2_{\ln\tau}$ is relatively close to the simulated values for all three values of $\sigma_Y$ (figure 3*c*). Since for $x \to \infty$, $\langle\tau\rangle \sim x$ and $\sigma^2_\tau \sim x$, and similarly for $\beta$, $\sigma^2_{\ln\tau}$ and $\sigma^2_{\ln\beta}$ tend to zero asymptotically.

The correlation coefficient, $\rho \equiv \sigma_{\ln\tau\ln\beta}/(\sigma_{\ln\tau}\sigma_{\ln\beta})$ is illustrated in figure 3(*e*). The first-order analytical correlation coefficient $\rho$ obtained from (28), (C 10) and (C 11) is essentially 1.0. Simulated $\rho$ varies relatively little with distance, increasing to an asymptotic value that ranges from approximately 0.88 to 0.98; larger $\sigma_Y$ yields smaller asymptotic values of $\rho$.

The relatively strong correlation between $\tau$ and $\beta$ is a consequence of their strong dependence on the fracture aperture, $b$, suggesting an approximate deterministic relationship between $\tau$ and $\beta$. In figure 4 we plot $\log(\tau/\tau_0)$ vs. $\log(\beta/\beta_0)$ covering the range of values that has been observed in simulations. The data are approximated by a straight line, indicating a power-law dependence, with the exponent of $\frac{3}{2}$, i.e. approximately $\beta \sim \tau^{3/2}$. The particular slope of $\frac{3}{2}$ in figure 4 is an artifact of the 'cubic law'. In fact, the zero-order approximation model which neglects the variability in $b$ and $\boldsymbol{\Omega}$ yields $\tau = x/c_0 b_G^2 \Omega$ and $\tau = x/c_0 b_G^3 \Omega$ where $\Omega \equiv \bar{\Omega}$ is the applied (uniform)

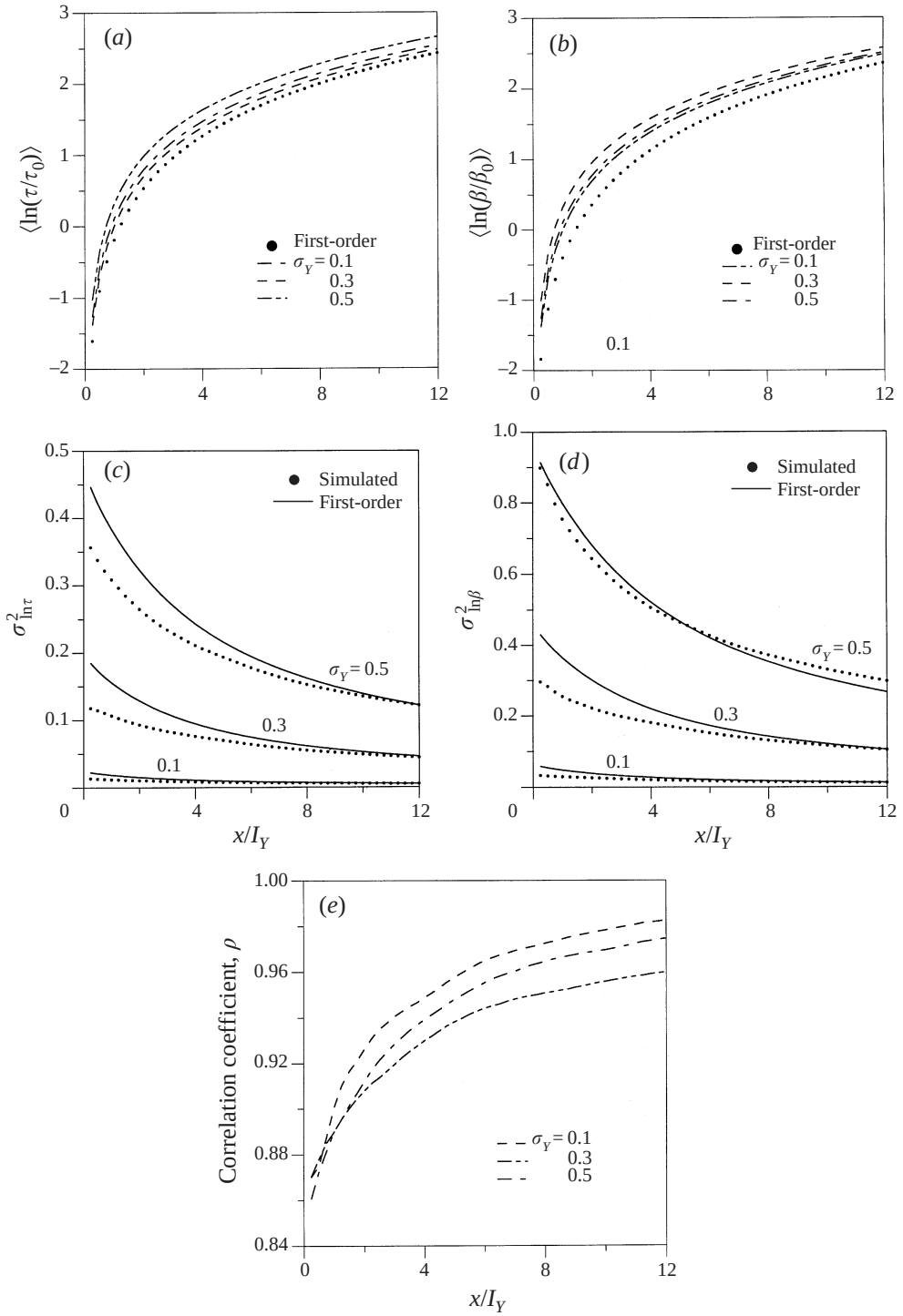


FIGURE 3. Comparison of $(\tau, \beta)$ statistical moments obtained from first-order analysis (eqs. (27)–(28) and eqs. (C 10)–(C 11)) and from numerical Monte Carlo simulations, as a function of the dimensionless distance, and for different $\sigma_Y$ : (*a*) $\langle \ln(\tau/\tau_0) \rangle$; (*b*) $\langle \ln(\beta/\beta_0) \rangle$; (*c*) $\sigma^2_{\ln\tau}$; (*d*) $\sigma^2_{\ln\beta}$; (*e*) correlation coefficient $\rho \equiv \sigma_{\ln\tau\ln\beta}/(\sigma_{\ln\tau}\sigma_{\ln\beta})$.

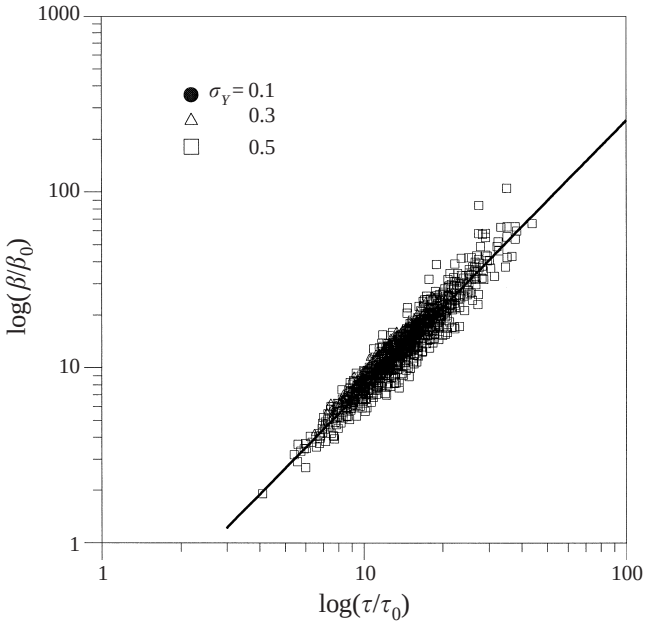


FIGURE 4. Simulated $\log(\tau/\tau_0)$ vs. $\log(\beta/\beta_0)$ data points for $\sigma_Y = 0.1$, $\sigma_Y = 0.3$ and $\sigma_Y = 0.5$, with the linear best fit which gives $\beta/\beta_0 = 0.23(\tau/\tau_0)^{3/2}$.

hydraulic gradient, and $b_G$ is the (uniform) half-aperture (Appendix C). Eliminating $b_G$ from these two expressions yields

$$\beta = \left(\frac{x}{c_0\,\Omega}\right)^{-1/2} \tau^{3/2} \quad \text{or} \quad \frac{\beta}{\beta_0} = \left(\frac{x}{I_Y}\right)^{-1/2} \left(\frac{\tau}{\tau_0}\right)^{3/2}. \tag{29}$$

The straight line in figure 4 yields $\beta/\beta_0 = 0.23\,(\tau/\tau_0)^{3/2}$; the factor 0.23 is closely approximated by $(x/I_Y)^{-1/2} = 0.29$ in (29). This indicates that although the flow dynamics as described by Reynolds lubrication equation (A 1) (Appendix A) strongly influences variability in $\tau$ and $\beta$, it influences the relationship between $\tau$ and $\beta$ less. If an alternative flow model is used which deviates from the cubic law, or a more general statistical model for $Y$ is considered, then the slope in figure 4 needs to be re-evaluated.

## 7. Illustration example: CDF for tracer mass recovery

In §4–5 we have solved the transport problem, explicitly accounting for the heterogeneity in the fracture aperture which directly controls advection and diffusion into the rock matrix, and thereby indirectly controls sorption in the matrix. In this Section we shall illustrate the effect of aperture variability on tracer transport, focusing on diffusive mass transfer by neglecting surface sorption ($K_a = 0$).

A typical problem in long-term assessment of tracer transport is to quantify how much of the tracer mass which enters fractured rock is eventually discharged from the rock. Here we solve this problem for a single fracture.

In the absence of decay, the mass recovered from a fracture is equivalent to the mass released into the fracture. However, in the case where decay is non-zero, the recovered mass will vary depending on the coupled processes of advection, diffusion

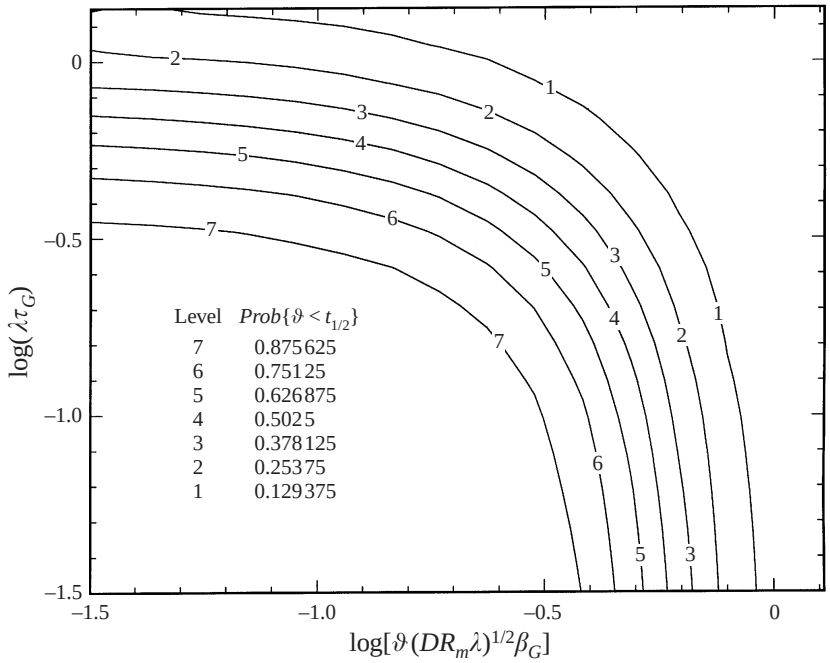


FIGURE 5. Surface plot of the probability $Prob\left\{\vartheta < t_{1/2}\right\}$ in the log-parameter space $\log\tau^*_G$,$\log\beta^*_G$, at $x/I_Y = 12$ for $\sigma_Y = 0.5$.

and sorption. Moreover, the mass recovered will vary in a random manner. We wish to illustrate the effect of aperture variability on the normalized zero-order temporal moment, $\mu \equiv m_0/\Delta M$, where $m_0$ is computed from (23). $\mu$ quantifies the fractional mass recovery, where $\mu = 1$ in the absence of decay (i.e. for $\lambda = 0$), otherwise $\mu < 1$. The specific case we shall illustrate is for $\widehat{\gamma}$ (22) (with $K_a = 0$) whereby

$$\mu = \exp\left[-(\tau + K_a\,\beta)\,\lambda - \beta\,\theta\,(DR_m\lambda)^{1/2}\right]. \tag{30}$$

The PDF of $\mu$ (30) is evaluated as

$$f(\mu) = \frac{1}{\mu}\int_0^{-\ln\mu} f_{\tau^*\beta^*}\left(\tau^*, -\ln\mu - \tau^*\right)\,\mathrm{d}\tau^*. \tag{31}$$

where dimensionless $\tau$ and $\beta$ are here defined as $\tau^* \equiv \lambda\tau$ and $\beta^* \equiv \beta\theta\,(DR_m\lambda)^{1/2}$. Based on the moments of $\tau$ and $\beta$ which are determined from simulations or analytically, we assume for illustrative purposes a log-normal joint PDF $f_{\tau\beta}$, and evaluate $f(\mu)$ from (31). Note that for $\tau$ and $\beta$ log-normal, the dimensionless geometric means are defined as $\tau^*_G \equiv \lambda\tau_G$ and $\beta^*_G \equiv \beta_G\theta\,(DR_m\lambda)^{1/2}$. In our following calculations, we shall use the geometric means $\tau_G$ and $\beta_G$, the log-variances $\sigma^2_{\ln\tau}$ and $\sigma^2_{\ln\beta}$, as well as the cross-covariance $\sigma_{\ln\tau\ln\beta}$, obtained from simulations at $x/I_Y = 12$ (figure 3*c–e*).

From $f(\mu)$ (31), the CDF is $\int_0^{\mu} f(\mu')\mathrm{d}\mu'$. The probability that $\mu > 0.5$ is quantified by $Prob\left\{\mu > 0.5\right\} = 1 - \int_0^{1/2} f(\mu')\mathrm{d}\mu'$. The subparticle residence time in the system, $\vartheta$, will depend on the combined effect of advection and mass transfer reactions. The significance of $Prob\left\{\mu > 0.5\right\}$ is in that it is equivalent to the probability of subparticle residence time in the fracture–rock matrix system relative to tracer half-life, i.e. we can write $Prob\left\{\mu > 0.5\right\} = Prob\left\{\vartheta < t_{1/2}\right\}$, where $t_{1/2}$ denotes half-life of the tracer.

In figure 5, $Prob\left\{\vartheta < t_{1/2}\right\}$ is presented as a surface plot in the dimensionless log-parameter space $\log\tau_G^*$, $\log\beta_G^*$, for low and high variability in the fracture aperture. The front between the low and high probability values is dispersed (figure 6), compared to a sharp front between regions of $Prob\left\{\vartheta < t_{1/2}\right\} = 0$ and $Prob\left\{\vartheta < t_{1/2}\right\} = 1$ for $\sigma_Y = 0$ where $\tau$ and $\beta$ are specified values. The general pattern of figure 6 reflects the fact that stronger decay and mass transfer result in greater mass loss and hence in greater values of $Prob\left\{\vartheta < t_{1/2}\right\}$, and vice versa for weaker decay and mass transfer.

## 8. Summary

A Lagrangian probabilistic model for reactive tracer transport in single rock fractures has been developed. The mass transfer reactions are diffusion into the rock matrix, sorption on fracture surfaces and/or infill (gauge) material, and sorption in the rock matrix. The model relates diffusive mass transfer to flow dynamics; hence, it generalizes on the one side models for non-reactive tracer transport based on the dynamics of fluid flow (e.g. Moreno *et al.* 1988; Tsang & Tsang 1989), and on the other side models for reactive transport where flow dynamics is not accounted for (e.g. Neretnieks *et al.* 1982; Neretnieks 1983; Moreno *et al.* 1985; Wels *et al.* 1994; Cvetkovic 1991). The proposed transport model rests on two key assumptions: diffusion into the rock matrix is one-dimensional, in the direction orthogonal to the fracture plane, and only advective transport is considered in the fracture.

A general Lagrangian deterministic solution of the transport problem is obtained in the Laplace domain and is given in (10). From the solution $\widehat{\gamma}$ (10), temporal moments can be computed and analysed statistically. For the case where $K_d^f = K_a/b$ and $K_a$ is uniform, we identified a single Lagrangian random variable, $\beta$, which controls the diffusive mass transfer into the rock matrix, as well as surface sorption. The probabilistic solutions are obtained based on the statistics of $\tau$ and $\beta$. In particular, the mean and variance of $\gamma$ are evaluated in (24)–(25), using the joint PDF $f_{\tau\beta}$. The PDF of the temporal moments can also be computed from the joint PDF $f_{\tau\beta}$. For quantifying the statistics of $\tau$ and $\beta$ we used the Reynolds lubrication equation (A 1), i.e. we assumed the 'cubic law' to be applicable locally. However, our general result is not restricted by the 'cubic law' model.

Expressions for the first few moments of $\tau$ and $\beta$ have been derived using first-order expansions, and compared to results of Monte Carlo simulations (figure 3). Analytical expressions appear robust for the range of variability in the fracture aperture considered. Simulation results indicate that $\langle\beta\rangle$ increases with increasing $\sigma_Y$, implying that diffusion into the rock matrix is in a statistical sense enhanced by increasing fracture heterogeneity. In view of its definition, $\beta$ has a stronger dependence on the aperture in comparison to $\tau$, and hence is more influenced by the variability in $b$.

We evaluated the probability of tracer residence time, $\vartheta$, in the fracture–rock system, relative to tracer half-life, $t_{1/2}$. The results illustrate the dispersion of $Prob\left\{\vartheta < t_{1/2}\right\}$ in the dimensionless parameter space which is a consequence of spatial variability in fracture aperture (figure 5). If heterogeneity is not accounted for, the transition between regions with probabilities 1 and 0 for $\vartheta < t_{1/2}$, is a sharp front.

Simulation results suggest a deterministic relationship between $\beta$ and $\tau$ (figure 4). A general power law is $\beta \sim \tau^m$. We found $m = \frac{3}{2}$ which is an artifact of the cubic law and is strictly applicable only for the conditions considered in the simulations. A zero-order approximation of the cubic law (which in effect neglects variability in the flow), also yields $m = \frac{3}{2}$. Thus flow dynamics has relatively small impact on the relationship between $\tau$ and $\beta$, although it strongly influences the variability of $\tau$ and

$\beta$ (figure 3). The framework presented can be used for identifying the exponent $m$ under flow conditions more general than those considered here.

The possibility of using a deterministic relationship $\beta \sim \tau^m$ would have important practical advantages in site characterization, as well as in safety assessment studies, for waste repositories in crystalline rocks. In particular, a deterministic relationship between $\tau$ and $\beta$ would imply that the estimation of $\beta$ in the field can be based entirely on the hydraulic and non-reactive transport properties of rock fractures, hence minimizing the need for time-consuming and costly reactive tracer tests. More comprehensive studies are required, however, before a model of the type $\beta \sim \tau^m$ can be used with confidence in field applications. Such studies (analytical and/or based on simulations similar to the ones presented here), should include one or several generalizations, such as modifying the flow model to account for deviations from the cubic law, implementing different statistical models for $b$, considering larger variances than $\sigma_Y = 0.5$, testing alternative boundary conditions for flow in fractures (e.g. radially converging and dipole configurations), etc.

The mean and variance of tracer discharge, (24)–(25) with (9), were derived by considering a single flow path through a fracture. A single flow path implies a source that is small compared to the heterogeneity integral scale. In applications, however, the source size will vary. Thus an important question for applications is how our results relate to tracer sources of finite extent. In order to quantify $\langle q \rangle$ that is consistent with the observable $q$ in single realizations for a finite source, we require analysis of 'relative' dispersion for reactive solute flux (Selroos 1995; Andricevic & Cvetkovic 1998). Details of a relative dispersion formulation of reactive transport in aquifers for the tracer mass flux are given in Andricevic & Cvetkovic (1998); this methodology can in principle be extended to reactive transport in fractures by incorporating the variability in $\beta$.

Transport problems in fractured rock are generally on large scales. For performance and safety assessment of waste repositories, for instance, the length scales from canisters to the biosphere are typically of the order of $10^3$ m. By comparison, the scale of a typical tracer source, for example, from one or several failed canisters, is percieved on the order of $10^0$ m, or less. Under such conditions, the potential transport path from a failed canister to the biosphere may be considered as a single advection flow path, transecting a number of rock fractures. $\tau$ (7) and $\beta$ (12) are then integral, random quantities from the canister to the biosphere. In order for the present results to be applicable in safety and performance assessment studies, transport in several fractures has to be serially connected; an analytical model for a network of fractures has recently been developed (Painter, Cvetkovic & Selroos 1998).

The authors wish to thank G. Dagan at Tel-Aviv University, A. Hautojärvi at the Technical Research Centre of Finland, L. Moreno and I. Neretnieks at the Royal Institute of Technology in Stockholm, for their helpful comments and suggestions which improved the original version of the manuscript. The support for this work has been provided by the Swedish Nuclear Fuel and Waste Management Co. (SKB) within the *Tracer Retention Understanding Experiment (TRUE)* programme, Äspö Hard Rock Laboratory, Sweden.

## Appendix A. Flow in rock fractures

The aperture $2b$ is a geometrical parameter that in principle can be measured in a fracture plane. In an appropriately designed experiment, the flow rate through a

fracture and the corresponding velocity can also be measured. Such experiments have been conducted in the laboratory, and results indicate that the fluid flow rate in fractures may under certain conditions be approximated as proportional to $b^3$ ('cubic law'), whereby the fluid velocity is proportional to $b^2$.

The governing equations for flow of an incompressible viscous fluid in a fracture are the Navier–Stokes and continuity equations. If steady-state conditions are assumed in a fracture bounded by two perfectly parallel and smooth plates, the flow equation is simplified as $\mu\nabla^2\boldsymbol{u} = \nabla P$ where $\boldsymbol{u}$ is the fluid velocity, $P = p + \rho g z$, $p$ is the pressure, $g$ is gravity acting in the vertical direction, $z$ is the vertical coordinate and $\mu$ is the fluid viscosity (e.g. Batchelor 1967). Integration of this equation with zero velocity at fracture surfaces yields a parabolic velocity profile for the $x$-component of the velocity, $u_x$, proportional to the pressure gradient.

The volumetric flow rate, $Q$ $[L^3T^{-1}]$ is obtained by integrating the velocity over the fracture aperture, as $Q = 2|\nabla P| wb^3/3\mu$ where $w$ is the width of the fracture; this expression is consistent with Darcy's law for flow in porous media. Comparison with Darcy's law indicates that $b^2/3$ corresponds to the permeability. From the permeability, the transmissivity $[L^2T^{-1}]$ is $2\rho g b^3/3\mu$, commonly referred to as the 'cubic law'. Averaging $u_x(x, y, z)$ and $u_y(x, y, z)$ over $z$, we obtain the components of the two-dimensional velocity vector $\boldsymbol{V}(x, y)$, $V_x$ and $V_y$, respectively.

By assuming that the cubic law is applicable locally, i.e. over an element $\mathrm{d}x \times \mathrm{d}y$ (figure 1), and invoking mass balance, the governing equation for $P$ is obtained in the form (Reynolds 1886; Zimmerman & Bodvarsson 1996)

$$\frac{\partial}{\partial x}\left[b^3(x, y)\frac{\partial P}{\partial x}\right] + \frac{\partial}{\partial y}\left[b^3(x, y)\frac{\partial P}{\partial y}\right] = 0. \tag{A 1}$$

It can be shown that the validity of (A 1) for flow in spatially variable fractures requires a more stringent condition on the flow rate as compared to flow between smooth, parallel plates (Zimmerman & Bodvarsson 1996). In addition to the restriction on the flow rate, some restrictions on the spatial rate of change of the aperture profile are required for (A 1) to be applicable (Zimmerman & Bodvarsson 1996). Equation (A 1), referred to as Reynolds lubrication equation, can be used for computing the pressure (head) field in a spatially variable fracture for specified boundary conditions. The fluid velocity, $\boldsymbol{V}$, is then proportional to the local pressure gradient and $b^2(x, y)$. Equation (A 1) has been used in several simulation studies of flow and transport in single fractures (e.g. Moreno *et al.* 1988; Tsang & Tsang 1989), and is also used in this study.

## Appendix B. Laplace solution

Laplace transform of the system (6) yields for zero initial condition

$$s\,\widehat{C} + \frac{\partial \widehat{C}}{\partial \tau} = \frac{\theta D}{b(\tau)}\left.\frac{\partial \widehat{C}_m}{\partial z}\right|_{z=0} - \lambda\,\widehat{C} - \alpha_f\,[K_d^f(\tau)\,\widehat{C} - \widehat{C}'], \tag{B 1a}$$

$$s\,\widehat{C}_m = D\frac{\partial^2 \widehat{C}_m}{\partial z^2} - \alpha_m\,(K_d^m\,\widehat{C}_m - \widehat{C}'_m) - \lambda\,\widehat{C}_m, \tag{B 1b}$$

$$s\,\widehat{C}' = \alpha_f\,[K_d^f(\tau)\,\widehat{C} - \widehat{C}'] - \lambda\,\widehat{C}', \tag{B 1c}$$

$$s\,\widehat{C}'_m = \alpha_m\,(K_d^m\,\widehat{C}_m - \widehat{C}'_m) - \lambda\,\widehat{C}'_m. \tag{B 1d}$$

Using (B 1*c*) and (B 1*d*) and substituting for $\widehat{C}'$ and $\widehat{C}'_m$ in (B 1*a*) and (B 1*b*), we get

$$\frac{\mathrm{d}\widehat{C}}{\mathrm{d}\tau} = \frac{\theta D}{b(\tau)} \left.\frac{\partial \widehat{C}_m}{\partial z}\right|_{z=0} - (\lambda + s) \left[1 + \frac{\alpha_f K_d^f}{s + \lambda + \alpha_f}\right] \widehat{C}, \tag{B 2a}$$

$$\frac{\partial^2 \widehat{C}_m}{\partial z^2} = \frac{s + \lambda}{D} \widehat{C}_m + \frac{(s + \lambda)\, \alpha_m K_d^m}{D\ (s + \lambda + \alpha_m)} \widehat{C}_m. \tag{B 2b}$$

The general solution of (B 2*b*) is

$$\widehat{C}_m = C_1 \exp\left[-z\,(D^{-1} G_m(s'))^{1/2}\right] + C_2 \exp\left[z\,(D^{-1} G_m(s'))^{1/2}\right], \tag{B 3}$$

where $C_1$ and $C_2$ are constants (with respect to $z$) to be determined from boundary conditions, and $G_m$ is defined in (11).

For zero flux boundary condition ($\partial C_m/\partial z = 0$) at $z = \zeta$, we get

$$C_1 = \frac{\widehat{C} \exp\left[2\,\zeta\,(D^{-1} G_m(s'))^{1/2}\right]}{1 + \exp\left[2\,\zeta\,(D^{-1} G_m(s'))^{1/2}\right]}, \tag{B 4a}$$

$$C_2 = \widehat{C} - C_1 = \frac{\widehat{C}}{1 + \exp\left[2\,\zeta\,(D^{-1} G_m(s'))^{1/2}\right]}. \tag{B 4b}$$

Thus

$$\left.\frac{\partial \widehat{C}_m}{\partial z}\right|_{z=0} = -\widehat{C}\, A(s')\,(D^{-1} G_m(s'))^{1/2}, \tag{B 5}$$

where $A$ is defined in (11).

For zero concentration boundary condition ($C_m = 0$) at $z = \zeta$, we get following similar steps as above

$$\left.\frac{\partial \widehat{C}_m}{\partial z}\right|_{z=0} = -\widehat{C}\, A^{-1}(s')\,(D^{-1} G_m(s'))^{1/2}. \tag{B 6}$$

Using (B 5) in (B 2) we get

$$\frac{\mathrm{d}\widehat{C}}{\mathrm{d}\tau} = -\widehat{C}\ \left[s'\,\tau + b^{-1}(\tau)\, A(s')\,\theta\,(D\, G_m(s'))^{1/2} + b^{-1}(\tau)\, G_f(s', \tau)\right], \tag{B 7}$$

and similarly for zero concentration, where $A$ is replaced by $A^{-1}$. Integration of (B 7) yields (10).

## Appendix C. First-order results

As a first step, we approximate the Lagrangian quantities by the Eulerian ones, for instance,

$$V_x\{x, \eta(x)]\} \approx V_x(x, 0), \tag{C 1}$$

where the mean hydraulic gradient, $\langle \boldsymbol{\Omega} \rangle$ is assumed parallel to $x$, i.e. $\langle \boldsymbol{\Omega} \rangle(\bar{\Omega}, 0)$.

We then write

$$\tau(x) = \int_0^x \frac{\mathrm{d}x'}{V_x(x', 0)}, \quad \beta(x) = \int_0^x \frac{\mathrm{d}x'}{V_x(x', 0) b(x', 0)}. \tag{C 2}$$

The expression for $\boldsymbol{V}$ based on the cubic law is

$$\boldsymbol{V}(x, y) = c_0\, b^2(x, y)\, \boldsymbol{\Omega}(x, y), \tag{C 3}$$

where $c_0$ $[L^{-1}\,T^{-1}]$ is a known constant. The approximate Lagrangian velocity is

$$V_x(x,0) = c_0\, b^2(x,0)\, \Omega_x(x,0). \tag{C 4}$$

For $b$ log-normally distributed we approximate (C 2) using (C 4), to obtain at first-order

$$\left.\begin{aligned} \tau(x) &= \frac{\tau_0}{I_Y}\int_0^x \mathrm{e}^{2Y}\,(1+\varpi)^{-1}\,\mathrm{d}x' \approx \frac{\tau_0}{I_Y}\int_0^x (1-2Y-\varpi)\,\mathrm{d}x', \\ \beta(x) &= \frac{\beta_0}{I_Y}\int_0^x \mathrm{e}^{3Y}\,(1+\varpi)^{-1}\,\mathrm{d}x' \approx \frac{\beta_0}{I_Y}\int_0^x (1-3Y-\varpi)\,\mathrm{d}x', \end{aligned}\right\} \tag{C 5}$$

where $\varpi \equiv \Omega_x'/\bar{\Omega} = (\Omega_x - \bar{\Omega})/\bar{\Omega}$, $\langle\varpi\rangle = 0$, and the normalization parameters are defined by

$$\tau_0 \equiv \frac{I_Y}{c_0\, b_G^2\, \bar{\Omega}}, \quad \beta_0 \equiv \frac{\tau_0}{b_G} = \frac{I_Y}{c_0\, b_G^3\, \bar{\Omega}}. \tag{C 6}$$

Note that a zero-order expansion yields $\tau/\tau_0 = x/I_Y$ and $\beta/\beta_0 = x/I_Y$; this is equivalent to the flow model where fracture aperture is approximated as uniform.

The first-order expressions for the moments $\sigma_\tau^2, \sigma_\beta^2$ and $\sigma_{\tau\beta}$ are

$$\left.\begin{aligned} \sigma_\tau^2 &\equiv \langle\tau^2\rangle - \langle\tau\rangle^2 = 2\left(\frac{\tau_0}{I_Y}\right)^2 \int_0^x (x-\xi)\,(4C_Y + 4C_{Y\varpi} + C_\varpi)\,\mathrm{d}\xi, \\ \sigma_\beta^2 &\equiv \langle\beta^2\rangle - \langle\beta\rangle^2 = 2\left(\frac{\beta_0}{I_Y}\right)^2 \int_0^x (x-\xi)\,(9C_Y + 6C_{Y\varpi} + C_\varpi)\,\mathrm{d}\xi, \\ \sigma_{\tau\beta} &\equiv \langle\tau\beta\rangle - \langle\tau\rangle\langle\beta\rangle = 2\,\frac{\tau_0\,\beta_0}{I_Y^2} \int_0^x (x-\xi)\,(6C_Y + 5C_{Y\varpi} + C_\varpi)\,\mathrm{d}\xi, \end{aligned}\right\} \tag{C 7}$$

where

$$C_{Y\varpi} \equiv \langle Y\,\varpi\rangle, \quad C_\varpi \equiv \langle\varpi\varpi'\rangle. \tag{C 8}$$

We use the methodology of Dagan (1989) to obtain

$$\left.\begin{aligned} C_{Y\varpi}(r') &= \sigma_Y^2\left[-\mathrm{e}^{-r'}\left(\frac{1}{r'^2} + \frac{1'}{r} + 1\right) + \frac{1}{r'^2}\right], \\ C_\varpi(r') &= \sigma_Y^2\left[\mathrm{e}^{-r'}\left(1 + \frac{2}{r'} + \frac{5}{r'^2} + \frac{9}{r'^3} + \frac{9}{r'^4}\right) - \frac{1}{2r'^2} - \frac{9}{r'^2}\right], \end{aligned}\right\} \tag{C 9}$$

where $r' \equiv r/I_Y$. Substituting (C 9) into (C 7) and integrating yields (28).

The simulation results are conveniently expressed as statistics of $\ln\tau$ and $\ln\beta$. For comparison between simulation and analytical results, we assume $\tau$ and $\beta$ as log-normally distributed. The log-moments are then computed as

$$\langle\ln\tau\rangle = \ln\langle\tau\rangle - \tfrac{1}{2}\,\sigma_{\ln\tau}^2, \quad \sigma_{\ln\tau}^2 \equiv \langle(\ln\tau)^2\rangle - \langle\ln\tau\rangle^2 = \ln\left[\left(\frac{\sigma_\tau}{\langle\tau\rangle}\right)^2 + 1\right], \tag{C 10}$$

and similarly for $\beta$; the joint log-moment is

$$\sigma_{\ln\tau\ln\beta} \equiv \langle\ln\beta\ln\tau\rangle - \langle\ln\beta\rangle\langle\ln\tau\rangle = \ln\langle\tau\beta\rangle - \langle\ln\tau\rangle - \langle\ln\beta\rangle - \tfrac{1}{2}\left(\sigma_{\ln\tau}^2 + \sigma_{\ln\beta}^2\right) \tag{C 11}$$

where $\langle\tau\rangle$, $\langle\beta\rangle$, $\sigma_\tau^2$, $\sigma_\beta^2$ and $\sigma_{\tau\beta}$ are given in (27) and (28).

## REFERENCES


Andricevic, R. & Cvetkovic, V. 1998 Relative dispersion for solute flux in aquifers. *J. Fluid Mech.* **361**, 145–174.

Batchelor, G. K. 1967 *An Introduction to Fluid Dynamics*. Cambridge University Press.

Bellin, A. & Rubin, Y. 1996 HYDRO_GEN: A spatially distributed random field generator for correlated properties. *Stoch. Hydrol. Hydraul.* **10**, 253–278.

Cvetkovic, V. 1991 Mass arrival of reactive solute in single fractures. *Water Resour. Res.* **27**, 177–183.

Cvetkovic, V., Cheng, H. & Wen, X. H. 1996 Analysis of nonlinear effects on advective tracer transport in heterogeneous aquifers using the Lagrangian statistics of travel time. *Water Resour. Res.* **32**, 1671–1680.

Cvetkovic, V. & Dagan, G. 1994 Transport of kinetically sorbing solute by steady random velocity in heterogeneous porous formations. *J. Fluid Mech.* **265**, 189–215.

Cvetkovic, V. & Dagan, G. 1996 Reactive transport and immiscible flow in geological media. 2 Applications. *Proc. R. Soc. Lond.* A **452**, 303–328.

Cvetkovic, V., Dagan, G. & Cheng, H. 1998 Contaminant transport in aquifers with spatially variable flow and sorption properties. *Proc. R. Soc. Lond.* A **454**, 2173–2207.

Dagan, G. 1984 Solute transport in heterogeneous porous formations. *J. Fluid Mech.* **145**, 151–177.

Dagan, G. 1989 *Flow and Transport in Porous Formations*. Springer, 465 pp.

Dagan, G. & Cvetkovic, V. 1996 Reactive transport and immiscible flow in geological media 1. General theory. *Proc. R. Soc. Lond.* A **452**, 285–301.

Dagan, G. & Fiori, A. 1997 The influence of pore-scale dispersion on concentration statistical moments in transport through heterogeneous aquifers. *Water Resour. Res.* **33**, 1595–1606.

Destouni, G. & Cvetkovic, V. 1991 Field-scale mass arrival of sorptive solute into the groundwater. *Water Resour. Res.* **27**, 1315–1325.

Hakami, E. 1995 Aperture distribution of rock fractures. PhD Thesis, Dept. of Civil and Env. Eng., Royal Inst. of Tech., Stockholm, Sweden.

Hakami, E. & Larsson, E. 1996 Aperture measurements and flow experiments on a single natural fracture. *Intl J. Rock Mech. Min. Sci. Geomech. Abstr.* **33**, 395–404.

MODFLOW/EM 1994 *The USGS Three Dimensional Ground Water Flow Model*. Maximal Engineering Software, Inc.

Moreno, L. & Neretnieks, I. 1993 Flow and nuclide transport in fractured media: The importance of the flow-wetted surface. *J. Contam. Hydrol.* **13**, 49–71.

Moreno, L., Neretnieks, I. & Eriksen, T. 1985 Analysis of some laboratory tracer runs in natural fissures. *Water Resour. Res.* **21**, 951–958.

Moreno, L., Tsang, Y. W., Tsang, C. F., Hale, F. V. & Neretnieks, I. 1988 Flow and tracer transport in a single fracture. A stochastic model and its relation to some field observations. *Water Resour. Res.* **24**, 2033–2048.

Neretnieks, I. 1980 Diffusion in the rock matrix: An important factor in radionuclide retardation? *J. Geophys. Res.* **85(B8)**, 4379–4397.

Neretnieks, I. 1983 A note on fracture flow dispersion mechanisms in the ground. *Water Resour. Res.* **19**, 364–370.

Neretnieks, I. 1993 Solute transport in fractured rock - Applications to radionuclide waste repositories. In *Flow and Contaminant Transport in Fractured Rock* (ed. J. Bear, C. F. Tsang & G. de Marsily). Academic.

Neretnieks, I., Eriksen, T. & Tähtinen, P. 1982 Tracer movement in a single fissure in granitic rock: Some experimental results and their interpretation. *Water Resour. Res.* **18**, 849–858.

Neuzil, C. E. & Tracy, J. V. 1981 Flow through fractures. *Water Resour. Res.* **17**, 191–199.

Painter, S., Cvetkovic, V. & Selroos, J. O. 1998 Transport and retention in fractured rock: Consequences of a power-law distribution for fracture lengths. *Phys. Rev.* E **57**, 6917–6922.

Reynolds, O. 1886 On the theory of lubrication. *Phil. Trans. R. Soc. Lond.* A **177**, 157–234.

Rubin, Y. & Dagan, G. 1988 Stochastic analysis of boundaries effects on head spatial variability in heterogeneous aquifers, 1. Constant head boundary. *Water Resour. Res.* **24**, 1689–1697.

Rubin, Y. & Dagan, G. 1989 Stochastic analysis of boundaries effects on head spatial variability in heterogeneous aquifers, 2. Impervious boundary. *Water Resour. Res.* **25**, 707–712.

Selroos, J. O. 1995 Temporal moments for non-ergodic solute transport in heterogeneous aquifers. *Water Resour. Res.* **31**, 1705–1712.

Snow, D. 1965 A parallel plate model of fractured permeable media. PhD Dissertation, University of California, Berkeley.

Taylor, G. I. 1921 Diffusion by continuous movements. *Proc. Lond. Math. Soc.* **20**, 196–212.

Tsang, Y. W. & Tsang, C. F. 1989 Flow channeling in a single fracture as a two-dimensional strongly heterogeneous permeable medium. *Water Resour. Res.* **25**, 2076–2080.

Wels, C., Smith, L. & Vandergraaf, T. T. 1994 Influence of specific surface area on transport of sorbing solutes in fractures: An experimental analysis. *Water Resour. Res.* **32**, 1943–1954.

Zimmerman, R. W. & Bodvarsson, G. S. 1996 Hydraulic conductivity of rock fractures. *Transport in Porous Media* **23**, 1–30.